Received Date:
Revised Date:
Accepted Date:
Article Type: Articles
Running Title: Parasite rearing temperature and disease

Parasite rearing and infection temperatures jointly influence disease transmission and shape seasonality of epidemics

Marta S. Shocket[1,4*], Daniela Vergara[1,5], Andrew J. Sickbert[1], Jason M. Walsman[1], Alexander T. Strauss[1,6], Jessica L. Hite[1,7], Meghan A. Duffy[2], Carla E. Cáceres[3], and Spencer R. Hall[1]

[1] Department of Biology, Indiana University, Bloomington, IN 47405 USA

[2] Department of Ecology and Evolutionary Biology, University of Michigan, Ann Arbor, MI 48109 USA

[3] School of Integrative Biology, University of Illinois at Urbana-Champaign, Urbana, IL 61801

* Corresponding Author: Marta S. Shocket, 650-723-5923, mshocket@stanford.edu

Manuscript type: Article

Manuscript received 16 December 2017; revised 3 April 2018; accepted 18 May 2018.

Corresponding Editor: Shelley E. Arnott

[4] Present address: Department of Biology, 371 Serra Mall, Stanford University, Stanford, CA 94305 (mshocket@stanford.edu)

[5] Present address: Department of Ecology and Evolutionary Biology, University of Colorado, Boulder, CO 80309 USA

[6] Present address: Department of Ecology, Evolution, and Behavior, University of Minnesota, St. Paul, MN 55108, USA

[7] Present address: Department of Biological Sciences, University of Nebraska at Lincoln, Lincoln, NE 68588, USA

ABSTRACT

Seasonal epidemics erupt commonly in nature and are driven by numerous mechanisms. Here, we suggest a new mechanism that could determine the size and timing of seasonal epidemics: rearing environment changes the performance of parasites. This mechanism arises when the environmental conditions in which a parasite is produced impact its performance—independently from the current environment. To illustrate the potential for 'rearing effects', we show how temperature influences infection risk (transmission rate) in a *Daphnia*-fungus disease system through both parasite rearing temperature and infection temperature. During autumnal epidemics, zooplankton hosts contact (eat) fungal parasites (spores) reared in a gradually cooling environment. To delineate the effect of rearing temperature from temperature at exposure and infection, we used lab experiments to parameterize a mechanistic model of transmission rate. We also evaluated the rearing effect using spores collected from epidemics in cooling lakes. We found that fungal spores were more infectious when reared at warmer temperatures (in the lab and in two of three lakes). Additionally, the exposure (foraging) rate of hosts increased with warmer infection temperatures. Thus, both mechanisms cause transmission rate to drop as temperature decreases over the autumnal epidemic season (from summer to winter). Simulations show how these temperature-driven changes in transmission rate can induce waning of epidemics as lakes cool. Furthermore, via thermally-dependent transmission, variation in environmental cooling patterns can alter the size and shape of epidemics. Thus, the thermal environment drives seasonal epidemics through effects on hosts (exposure rate) and the infectivity of parasites (a rearing effect). Presently, the generality of parasite rearing effects remains unknown. Our results suggest that they may provide an important but underappreciated mechanism linking temperature to the seasonality of epidemics.

KEYWORDS

Daphnia, disease ecology, disease seasonality, fungal disease, infectious disease, *Metschnikowia*, rearing effect, seasonal epidemics, temperature, thermal ecology, trans-host effect, transmission rate

INTRODUCTION

Disease outbreaks often erupt at the same time each year (Altizer et al. 2006). However, many potential drivers of disease change synchronously as these seasonal epidemics wax and

wane. This synchronization complicates the search for environmental factors that drive the dynamics of seasonal outbreaks (Pascual and Dobson 2005, Altizer et al. 2006). Nonetheless, many mechanisms contribute to the seasonality of infectious diseases, including influxes of susceptible hosts, changes in contact rates due to host behavior, changes in host immunity, influence of climate on free-living parasite stages in the environment, and climate-driven changes in vector abundance and vector and/or parasite physiology (Altizer et al. 2006, Grassly and Fraser 2006). We argue here for a new mechanism: rearing environment (i.e., during the previous infection) can change key traits of parasites in the subsequent infection—independently from effects of the current environment. Through these parasite 'rearing effects,' seasonal environments can alter traits that shape epidemics.

This idea emerges from previous work on trans-generational or maternal effects that generate phenotypic plasticity in host traits and influence disease interactions. ('Plastic' means the environment changes phenotypes without evolution). For example, offspring susceptibility and infection severity can depend on maternal exposure to parasites (Mitchell and Read 2005, Sadd et al. 2005, Moret 2006, Ben-Ami et al. 2010, Holeski et al. 2012), food resources (Mitchell and Read 2005, Ben-Ami et al. 2010, Boots and Roberts 2012, Garbutt et al. 2014), and temperature (Garbutt et al. 2014). Typically, the relevance of these effects on hosts is couched evolutionarily (i.e., plasticity might weaken parasite-mediated selection, thereby inhibiting evolutionary responses to disease: Lazzaro and Little 2009, Wolinska and King 2009). Plasticity in parasite traits is less-studied, and usually considered as a function of the current host environment (e.g., Mideo and Reece 2012). However, the rearing environment experienced by a parasite in a previous host can impact its performance in the subsequent host. These 'rearing effects' or 'trans-host effects' on parasites have arisen in a handful of systems in which the performance of a parasite depends on host resources (Tseng 2006, Little et al. 2007, Cornet et al. 2014) or host genotype (Searle et al. 2015) in the previous infection. These effects represent a biologically distinct mechanism for generating plasticity in parasite traits. Accordingly, their independent influence on disease interactions arises as long as (1) environmental conditions vary over some spatio-temporal scale and (2) key parasite traits (like infectivity) respond plastically to environmental conditions (like temperature) during prior infection. For rearing effects to shape the dynamics of seasonal epidemics, parasites must also reproduce and spread repeatedly during epidemics as the environment changes seasonally.

Here, we illustrate how a thermal rearing effect on parasite infectivity helps shape the size and timing of seasonal epidemics. During autumnal epidemics, zooplankton hosts and fungal parasites encounter each other in a gradually cooling thermal environment. A single infection cycle lasts 10-20 days; hence, as the epidemics progress from late summer to early winter, the parasite produces spores at very different temperatures (from approximately 27° down to 10°C). A rearing effect emerges because the temperature of parasite production influences their infectivity (also called per spore susceptibility) in the next host. However, temperature also influences other components of infection risk. For example, temperature controls the foraging rate of this ectothermic host. Since hosts eat spores, exposure becomes a thermally dependent trait (Hall et al. 2006, 2007, Shocket et al. 2018). Furthermore, spore infectivity itself may also depend on temperature at the time of exposure and during the new infection. Thus, any quantitative evaluation of thermal rearing effects on parasites must distinguish them from the other effects of temperature during exposure and infection. To address this challenge, we combine experiments and mathematical models designed to separate distinct effects of temperature on infection risk, aka transmission rate (as encouraged generally by McCallum et al. 2017): (1) temperature on host exposure (foraging), (2) rearing temperature on parasite infectivity, and (3) all other effects of temperature on parasite infectivity during exposure and infection.

Our investigation shows that parasite rearing temperature and exposure/infection temperature jointly influence disease transmission, and together they can drive the trajectory of seasonal epidemics. We present methods and results of three complementary analyses. First, in *Temperature-Dependence of Transmission: Experiments & Model*, we measured the effects of temperature on foraging rate and spore infectivity. We then quantitatively separated the three thermal effects (described above) by fitting a mechanistic model of transmission rate to the experimental data. The foraging rate of hosts (and, hence, exposure rate to spores) was higher at warmer temperatures. Additionally, spore infectivity was primarily driven by a pronounced thermal rearing effect: spores reared at warmer temperatures were much more infectious. Second, in *Field Test: Infectivity Assay,* a follow up experiment revealed that field-collected spores became less infectious as lakes cooled. Hence, the rearing effect detected in lab also arose in nature. Third, in *Simulations of Temperature-Explicit Epidemics*, we built a mathematical model of seasonal disease dynamics at the population level. Because the model lets us turn

specific thermal mechanisms on or off, it illustrates the separate thermal effects of rearing vs. exposure during autumnal cooling. Then, armed with the complete transmission model, more simulations linked different patterns of cooling to variation in the size and timing of seasonal epidemics. Thus, we identify and quantify a thermal rearing effect on parasite infectivity, confirm its relevance in the field, and illustrate its quantitative importance (alongside host exposure) in simulated epidemics.

STUDY SYSTEM

The parasite (*Metschnikowia bicuspidata*, hereafter, 'fungus') is a virulent ascomycete yeast (Ebert 2005). The host (*Daphnia dentifera*; hereafter 'host') is the dominant zooplankton grazer in many freshwater, temperate lakes across the Midwestern United States (Tessier and Woodruff 2002). During epidemics, infection prevalence can reach up to 60% (Hall et al. 2010, Penczykowski et al. 2014a). Hosts become infected when they filter-feed and inadvertently consume fungal spores. Thus, exposure rate is proportional to foraging rate (Hall et al. 2007). Once ingested, the needle-like spores pierce through the host's gut wall, entering the body cavity. The fungal conidia replicate in the host hemolymph before producing the next generation of spores (Metschnikoff 1884, Green 1974). When the host dies 10 – 20 days post-infection, spores are released into the water column where new hosts can consume them (Ebert 2005). Previous studies have not found genetic variation between populations via sequencing (Wolinska et al. 2009, Searle et al. 2015) or lab experiments measuring parasite traits (Duffy and Sivars-Becker 2007, Auld et al. 2014, Searle et al. 2015). However, spore infectivity responds plastically to host genotype (Searle et al. 2015).

The seasonality of epidemics motivates our focus on temperature. Fungal epidemics (defined in our system as infection prevalence >1% sustained for at least 2 weeks) typically begin in late summer or early fall (August – October) and wane in late fall or early winter (November – December; Fig 1A; Hall et al. 2011, Penczykowski et al. 2014a). During this time period, lake water temperature declines from approximately 27°C to 10°C (Fig. 1A, Appendix S1: Fig. S4). Thus, hosts and parasites encounter each other in a thermal environment that cools gradually. This natural history creates the opportunity for a pronounced thermal rearing effect if the temperature at which spores are produced impacts their performance. Additionally, hosts could encounter spores made in either similar or warmer temperatures. If most spores are

consumed or lost quickly after release, hosts are exposed to spores reared recently in a similar thermal environment. Alternatively, if spores remain in the water column for an extended time, hosts will encounter spores reared in a warmer past environment (on average). However, a rearing effect could impact parasite infectivity regardless of the presence or absence of such a temperature lag because it exerts a unique biological effect. Other traits that influence the spread of this fungus also change plastically with temperature (e.g., demographic traits of hosts, production of spores, and exposure rate; see Hall et al. 2006, Shocket et al. 2018). Therefore, seasonal dynamics of epidemics could depend on a thermal rearing effect coupled with the thermal responses of these other traits.

TEMPERATURE-DEPENDENCE OF TRANSMISSION: EXPERIMENTS & MODEL

Experimental Methods

Foraging Assay

We collected foraging rate data across gradients of temperature and host body size (L; Shocket et al. 2018). Foraging rate in *Daphnia* depends on both (Kooijman 2009), and our analysis requires estimates of foraging rate for two different body sizes (large adult L = 1.5 mm for the transmission model and population average L = 0.85 for simulations of epidemics). To quantity foraging, we used standard methods that compare the fluorescence of ungrazed and grazed algae (Sarnelle and Wilson 2008, Penczykowski et al. 2014b). See Appendix for detailed methods. Hosts were cultured at 16, 18, 21, 24, and 27°C. The assay used individuals from each temperature that spanned a size gradient including small juveniles, large juveniles, and adults. We fit the function for temperature- and size-dependent foraging rate (eq. 1, below) using maximum likelihood estimation via the 'bbmle' package (Bolker and R Development Core Team 2017) in R (R Core Team 2017). We generated 95% confidence intervals for the function coefficients by bootstrapping 10,000 samples.

Infection Assay

We measured transmission rate (β) at factorial combinations of parasite rearing (T_R) and exposure/infection (T_{EI}) temperatures using an infection assay. We reared spores at four temperatures (T_R = 15, 18, 20, and 22°C) and used those spores to infect new hosts at five temperatures (T_{EI} = 15, 18, 20, 22, and 25°C) for 20 total rearing temperature-exposure/infection

temperature combinations. This design was necessary to quantify the rearing effect independently of the effects of exposure/infection temperature. See Appendix for detailed methods and a discussion on experimental design for incorporating and measuring rearing effects. We cultured a cohort of neonate offspring for five days at 20°C (to control for body size at parasite exposure). On day 6 (average L = 1.5 mm), hosts were transferred to their temperature treatments and exposed to spores for 24 hours. We visually diagnosed hosts (20-50X) for infection 10-18 days post-exposure (depending on temperature). For each treatment, we used maximum likelihood to estimate the transmission rate from the proportion infected. We generated 95% confidence intervals for the transmission rate at each temperature combination by bootstrapping 10,000 samples.

Formation of the model

We built a mechanistic model of transmission rate as a function of both parasite rearing temperature (T_R) and exposure/infection temperature (T_{EI}; see Fig 1B). Transmission rate (β) is the product of foraging rate of hosts (f, since hosts encounter spores while foraging) and per spore infectivity (u). In the model, foraging rate of hosts depends only on exposure/infection temperature. In contrast, spore infectivity depends on both parasite rearing temperature and exposure/infection temperature. The rearing temperature determines spores' baseline infectivity. The exposure/infection temperature also influences the probability of successful infection via other effects on host and parasite physiology.

We fit the transmission model using data from the two assays described above. With data from the foraging assay, we modeled foraging rate (i.e., exposure rate) calculated for individual hosts as an Arrhenius function of exposure/infection temperature (T_{EI}) and a power function of body length of hosts (L):

$$f(T_{EI}, L) = L^{\gamma} \cdot \hat{f} \cdot e^{T_A\left(\frac{1}{T_{Ref}} - \frac{1}{T_{EI}}\right)} \quad \text{eq. 1}$$

with normally distributed errors. This size- and temperature-dependent foraging rate $f(T_{EI}, L)$, depends on body length (L) raised to a power coefficient (γ), the size-specific foraging rate ($\hat{f}$) at a reference temperature (T_{Ref} = 20°C), and an Arrhenius coefficient (T_A) governing how steeply foraging scales with temperature.

We used data from the infection assay to estimate transmission rate (β) at factorial

combinations of parasite rearing temperature (T_R) and exposure/infection temperature (T_{EI}). We calculated the spore infectivity (u) at each temperature combination [$u(T_{EI,}T_R)$] by dividing our point estimate of transmission rate, $\beta(T_{EI,}T_R)$, by the value of the foraging rate function for large adult hosts (infection assay average L = 1.5 mm) at the exposure/infection temperature [$f(T_{EI}, L$ = 1.5 mm)]. See Appendix for detailed methods. Spore infectivity, then, is:

$$u(T_{EI}, T_R) = \frac{\beta(T_{EI},T_R)}{f(T_{EI},1.5)} \quad \text{eq. 2}$$

This function (eq. 2) generates a 3D surface showing how spore infectivity depends on T_R and T_{EI}. We fit a linear plane to this 3D surface in R. We generated 95% confidence intervals for the slope coefficients using the bootstrapped values for foraging and transmission rates.

Results

Foraging rate (f) increased with temperature (T_{EI}) and host body length (L; Appendix S1: Table S1, Fig 2A,B). Since hosts encounter spores while foraging, they contact more spores in warmer environments. Thus, for a constant density of spores, exposure should decrease over the epidemic season as lakes cool.

Parasite rearing temperature (T_R) and exposure/infection temperature (T_{EI}) had opposing, linear effects on spore infectivity (u). Spore infectivity increased strongly with rearing temperature ($p < 0.0001$, slope $\alpha_R = 9.0 \times 10^{-5}$; light grey arrows in Fig 2C). However, it decreased (less strongly) with exposure/infection temperature ($p < 0.0001$, slope $\alpha_{EI} = -4.9 \times 10^{-5}$; dark grey arrows in Fig 2C). Based the slopes, the positive rearing effect on infectivity was 1.83 times larger than the opposing negative effect of exposure/infection temperature. Along with the linear model intercept ($\alpha_I = -0.011$), these slopes define the plane that describes how spore infectivity depends on both temperatures (Fig 2C).

While the factorial combination of temperatures is necessary to fit the transmission model, not all combinations of rearing (T_R) and exposure/infection temperatures (T_{EI}) occur in nature. For instance, during epidemics, if most spores are consumed shortly after their production, T_R and T_{EI} are approximately equal. In that scenario, spore infectivity (u) net increases with temperature, and therefore net decreases over time as lakes cool (following the dashed arrow in Fig 2C). Alternatively, T_R could lag behind T_{EI} if spores made in warmer conditions persist in the environment for a while. Still, T_R and T_{EI} are closely linked at the seasonal scale (since both start high and decrease simultaneously). Thus, we still expect spore

infectivity to decrease over time at the seasonal scale. (We address the potential lag between temperatures below: see *Simulations of Temperature-Explicit Epidemics* and *Discussion.*)

Transmission rate (β) estimated from the infection assay showed a complex relationship to parasite rearing and exposure/infection temperatures (solid lines and x-axis in Fig 2D, respectively). The model readily reproduced this pattern (dashed lines in Fig 2D) from the product of adult foraging rate (Fig 2B) and spore infectivity (Fig 2C), particularly the strong rearing effect. First, colder rearing temperature caused large drops in infectivity, regardless of exposure/infection temperature (i.e., differences in contour means in Fig 2C): spores made in colder conditions are less infectious. Then, transmission rate increased with exposure/infection temperature only when spores were reared in warmer conditions (e.g., 22°C, dark grey contours); the relationship flattened as rearing temperature dropped to colder temperatures (e.g., 15°C, light grey contour).

This complicated relationship between transmission rate (β) and exposure/infection temperature (T_{EI}) arose because rearing temperature (T_R) alters the net balance between two opposing influences of T_{EI} (Fig 2C, Table 2). On the one hand, T_{EI} exponentially increases host foraging (f) and contact with spores (Fig 2B); on the other, it simultaneously linearly decreases spore infectivity (u). When baseline spore infectivity is high (from warm T_R), it enhances the positive effects of T_{EI}, causing either high transmission (for the exponential effect on foraging when T_{EI} is warm) or medium transmission (for the linear effect on infectivity when T_{EI} is cool). When baseline spore infectivity is low (from cool T_R), it enhances the negative effects of T_{EI}, causing uniformly low transmission rate in combination with any T_{EI}. Overall, transmission rate is highest when rearing temperature and exposure/infection temperature are both warm, because hosts consume many spores with high baseline infectivity. These conditions resemble the start of fungal epidemics in late summer. Thus, transmission rate should decrease over the epidemic season as lakes cool.

FIELD TEST: INFECTIVITY ASSAY

Methods

Is the parasite rearing effect in the lab experiment relevant in nature? To answer this question, we tested whether rearing temperature (T_R) influenced infectivity (u) of spores collected from natural epidemics. We sampled epidemics in three lakes on November 9th and 23rd

2015 (Clear, Gambill, and Scott: Greene and Sullivan Counties, Indiana, USA). At both visits, we measured water temperature of each lake at 1 meter intervals with a Hydrolab multiprobe (Hach Environmental) and calculated the average temperature of the (unstratified) water column. The average temperature among the lakes was 13.7°C (+/- 0.50°C SE) on November 9th and 10.1°C (+/- 0.49°C SE) on November 23rd, a 3.6°C difference over fourteen days (~1 parasite generation). On each lake-date, we collected a zooplankton sample (13 cm diameter Wisconsin net with 153 µm mesh). After visually identifying infected hosts, we collected and homogenized ~30 hosts and quantified their spores (at 200X, with a hemocytometer). The spores from November 9th were diluted in filtered lake water and stored in open beakers at 15°C until the assay date. Spores retain their infectivity over this time scale in an oxygenated environment (unpublished data).

We used these field-collected spores in an infection assay. See Appendix for detailed methods. On November 25th, we exposed six-day-old large, adult hosts to spores. The assay was conducted at one exposure/infection temperature (21°C). Ten days later, we diagnosed the infection status of hosts and calculated the proportion infected for each spore treatment. We estimated transmission rates (β) according to eq. S6 in Appendix S1. Since the exposure/infection temperature (T_{EI}) was constant, differences in β stem from differences in spore infectivity (u; see Fig. 1B). We used randomization tests to determine if spore infectivity decreased in each lake. For each lake, spore-date was randomly shuffled (without replacement) among individual hosts 10,000 times. For each simulation, we estimated the transmission rate for both 'spore-dates' and subtracted to calculate the difference. These calculations created a distribution of expected values due to random chance. We used the inverse quantile function in R to assign a p-value to the observed difference in transmission rates based on these distributions.

Results

Spores collected from natural epidemics declined in infectivity as temperature dropped. More specifically, spore infectivity (measured as differences in transmission rate [β]) significantly decreased in two of three lakes (Fig. 3; Gambill $p < 0.0001$, Clear $p = 0.0024$). In the third lake, infectivity was already very low on the first date. Thus, although infectivity decreased, we did not have enough power to detect a significant difference (Scott $p = 0.16$).

SIMULATIONS OF TEMPERATURE-EXPLICIT EPIDEMICS

Methods

How might these thermal effects impact disease outbreaks at the population level? To answer this question, we used a mathematical model to study the relative contributions of foraging rate, $f(T_{EI})$, and spore infectivity, $u(T_{EI},T_R)$, during simulated epidemics. We also evaluated how variation in cooling scenarios regulates the trajectory and size of epidemics. In this population model, traits of host and parasite (i.e., model parameters) vary as functions of temperature (modified from Shocket et al. 2018 to include rearing temperature and omit algal food resources). The model, written without traits as functions of temperatures for visual clarity, is (see also Tables 1 and Appendix S1: Table S1):

$$\frac{dS}{dt} = b(1 - c(S + I))(S + I) - dS - ufSZ \quad \text{eq. 3a}$$

$$\frac{dI}{dt} = ufSZ - d_i I \quad \text{eq. 3b}$$

$$\frac{dZ}{dt} = d_i I\,\sigma - mZ - f(S + I)Z \quad \text{eq. 3c}$$

$$T_{EI}(t) = \frac{T_{max} - T_{min}}{1 + R^{t-D}} + T_{min} \quad \text{eq. 3d}$$

$$\frac{dT_R}{dt} = \frac{d_i I\,\sigma(T_{EI} - T_R)}{Z} \quad \text{eq. 3e}$$

Susceptible hosts (S, eq. 3a) increase via births from susceptible and infected (I) classes; per capita birth rate drops from its maximum, b, due to density-dependence parameter (c). Parasites have no effect on birth rate (identical b for both classes). Susceptible hosts decrease at background death rate (d) and become infected after consuming fungal spores (Z) at foraging (exposure) rate (f) that have spore infectivity (u). Infected hosts (eq. 3b) increase from infection and die at virulence-elevated rate d_i. Dead infected hosts release spores (eq. 3c) at spore yield (σ). Spores are lost at a background rate (m) and are removed by the foraging of susceptible and infected hosts.

Exposure/infection temperature (T_{EI}, eq. 3d) is the current water temperature, which is seasonally forced to decrease sigmoidally over time (t; see Fig 4A for example). It starts at a constant high temperature (T_{max}), decreases during autumnal cooling, and plateaus at a cold temperature (T_{min}). In this function, D is the day when temperature reaches the midpoint of cooling, and R controls the cooling rate (higher R means faster cooling). To avoid extending the transmission model to values colder than those used to parameterize it, we set T_{min} = 15ºC for all

simulations (although temperature drops well below 15°C in nature). T_{EI} is the sole determinant of all temperature-dependent traits (Appendix S1: Table S1) except spore infectivity (u). Spore infectivity also depends on the rearing temperature (T_R, eq. 3e) of spores. As lakes cool over time, new spores released into the environment are reared at cooler temperatures. To account for this dynamic process, the model tracks the mean rearing temperature of all spores in the environment (see Appendix for derivation). Mean spore rearing temperature changes with inputs of new spores ($d_i\, I\, \sigma$), weighted by the difference between the rearing temperature of new spores and the mean rearing temperature of old spores (T_{EI} - T_R). This cooling of T_R is slowed by higher densities of older spores (Z) that were reared at warmer temperatures but remain in the environment. Together T_{EI} and T_R determine spore infectivity (u). This modeling approach allows us to incorporate the rearing effect on infectivity and to quantify the lag between current water temperature and mean rearing temperature.

We used the model to quantify the contribution of host foraging rate (f) and spore infectivity (u) to decreasing disease transmission over the epidemic season. We simulated epidemics where both traits were held constant, each trait varied alone, and both traits varied with the appropriate temperatures. Then, we quantified how variation in cooling scenarios could influence epidemic size and the timing of peak prevalence. Lakes vary in their seasonal cooling patterns due to differences in habitat structure (for example, maximum depth, Appendix S1: Fig. S4A). For a given lake, inter-annual variation in the timing and rate of cooling is controlled by larger-scale climate variation (for example, Appendix S1: Fig. S1B). Thus, we varied 1) starting temperature (the high ceiling, T_{max}), 2) start date of cooling (D), and 3) steepness of cooling rate (R).

All simulations began with low infection prevalence (1%) to mimic the typical seasonal pattern we observe in nature (small initial start). We parameterized host foraging rate (eq. 1) with a typical average body length for these populations (L = 0.85 mm, unpublished data). Other traits (host birth rate [b], death rates of uninfected [d] and infected hosts [d_i], and spore yield [σ]) varied with current water temperature (T_{EI}) according to Table S1 (Shocket et al. 2018). The density-dependence of birth rate (c) and loss rate of spores (m) did not vary with temperature.

Results

In a typical cooling scenario (Fig. 4A), the temperature-dependence of foraging rate (f)

and spore infectivity (u) both lowered transmission rate (Fig. 4B) and infection prevalence (Fig. 4C). The difference between the mean parasite rearing temperature (T_R) and the current water temperature (T_{EI}) was negligible compared to the seasonal shifts in both temperatures. The maximum difference was ~0.17°C, because lakes cool gradually as spores are gained and lost. (Larger lags are possible given the plankton-like parameters used, but require large, sudden, and unrealistic changes in temperature: see Appendix S1: Fig S3.) Even though simulated T_{EI} and T_R closely tracked each other, both still strongly influenced epidemic size (current water temperature via host foraging rate and spore infectivity; rearing temperature via spore infectivity). Foraging rate alone had a larger effect on epidemic size than spore infectivity alone (as parameterized here, a 17% vs. 36% reduction in epidemic size [area under the prevalence curve]). Combined, both factors produced an even smaller epidemic (a 47% reduction as parameterized here) that qualitatively matches the seasonal waning of epidemics typically observed in nature (for example, in Fig 1A).

Different scenarios of lake cooling (determined by parameters of the T_{EI} function, eq. 3d: T_{max}, D, R), changed epidemic size and timing of peak prevalence. When lakes began the epidemic season with a warmer temperature (higher T_{max}), epidemics were larger (Fig 5A,B,C). However, epidemics reached their peak (maximum prevalence) latest in the season at intermediate starting temperatures. When the onset of cooling was delayed (higher D), epidemics were larger and peaked later in the season (Fig 5D,E,F). When lakes cooled faster (higher R) epidemics reached a higher peak prevalence, but total epidemic size remained fairly consistent, because prevalence also decreased more quickly (Fig 5G,H,I). For most of the range of R, the timing of peak prevalence changed little. Thus, cooling rate, R, had relatively small effects on epidemic properties compared to the other two parameters (T_{max} and D).

The patterns of these two epidemic properties (epidemic size and peak timing) have simple or complex explanations, respectively. The mechanistic link between cooling parameters and epidemic size is straightforward: warmer temperatures elevate transmission rate (β) via the effects on host exposure and spore infectivity. Thus, more time spent at higher temperatures (via higher T_{max}, later D, or steeper R) results in larger epidemics. However, the relationship between epidemic size and peak timing of epidemics is complex: epidemic size and date of peak prevalence can be either positively correlated (Fig 5F) or exhibit different relationships in different parts of parameter space (Fig 5C,I).

We dissect these relationships in detail in Appendix S1 (Fig. S4) but briefly summarize them here. The timing of peak prevalence is strongly influenced by the attracting interior, epidemic equilibrium (when temperatures are warmer and transmission rate is higher) or the attracting boundary, disease-free equilibrium (when conditions are colder and transmission rate becomes too low to support epidemics). The interior equilibrium contains the density of susceptible hosts, S^* (which is the minimal host requirement of the parasite: the lowest density of susceptible hosts required to maintain the epidemic) and the density of infected hosts, I^*. As epidemics grow, the parasite depletes susceptible hosts towards this minimal host requirement, S^*. However, cooling raises S^* (and lowers I^*). That relationship between the burn-through of S by the parasite (from infection) vs. the increase in minimal requirements (S^*) from cooling depends on transmission rate, the trait made so thermally sensitive from both foraging and rearing effects of temperature. The transmission-mediated burn-through varies among cooling scenarios, and lays at the heart of these varying relationships. After epidemics charge past this interior equilibrium (with infection depleting S, increasing I), epidemics peak and then wane with cooling. During that waning, transmission rate becomes too low to support epidemics (i.e., parasite losses exceed gains from new infections). However, it takes time for epidemics to coast towards elimination.

DISCUSSION

Can parasite rearing effects influence the outcome of host-parasite interactions? A handful of lab experiments show that the conditions in which a parasite is made can affect its performance in a subsequent infection (Tseng 2006, Little et al. 2007, Cornet et al. 2014). However, models of disease spread through populations rarely incorporate this type of parasite plasticity, and little is known about its impacts in naturally occurring epidemics. Here, we show how rearing temperature and exposure/infection temperature of parasites jointly influence transmission rate in a zooplankton-fungus disease system. Temperature effects on transmission matter in this system because hosts encounter parasites in a gradually cooling (autumnal) thermal environment.

To quantify the thermal rearing effect, we combined three modes of inference. First, we built and parameterized a mechanistic model of transmission rate (β) with experimental data. We found that higher temperatures increase transmission rate because higher exposure/infection

424 temperature elevates host foraging (and exposure to spores; *f*) and higher parasite rearing
425 temperature elevates spore infectivity (*u*). Therefore, transmission rate drops sharply over the
426 epidemic season, in part because cooler conditions result in lower quality spores. Second, we
427 verified the thermal rearing effect in nature: warmer-reared spores taken from lakes were more
428 infectious than colder-reared spores (in two of three lakes, with a trend in the other). Finally,
429 simulations demonstrate that these temperature-driven changes in transmission rate can explain
430 why epidemics become larger when they start warmer (Shocket et al. 2018) and wane as lakes
431 cool. The population model predicts that most spores are reared recently (i.e., rearing
432 temperature ≈ exposure/infection temperature) because lakes cool gradually as spores turn over
433 quickly. Nonetheless, rearing temperature still impacts disease transmission because it
434 independently elevates infection risk when warm and depresses it when cool. Hence, by
435 determining parasite quality, thermal rearing effects present a separate biological mechanism,
436 distinct from influence of current temperature on exposure (foraging) and infectivity.
437 Furthermore, variation in cooling patterns can alter epidemic size and timing. Thus, rearing
438 temperature and exposure/infection temperature jointly alter infection risk and influence the
439 seasonality of epidemics.

440 The plasticity of spore infectivity (*u*) is determined by a tug of war between rearing
441 temperature and exposure/infection temperature. Spore infectivity increased with rearing
442 temperature, T_R, so warm-reared spores were more infectious than cold-reared spores (for both
443 lab-reared and field-collected specimens). Although we can quantify this rearing effect, we
444 cannot yet explain its underlying mechanism. Conversely, higher temperature during exposure
445 and infection, T_{EI}, lowered spore infectivity. This effect might stem from enhancement of the
446 host immune system in warmer but not overly stressful temperatures (as seen in Ouedraogo et al.
447 2003, Adamo and Lovett 2011, Fuller et al. 2011, Triggs and Knell 2012; but see also Linder et
448 al. 2008, Murdock et al. 2012). Host immune cells phagocytose spores of this parasite
449 (Metschnikoff 1884, Green 1974) and can even clear infection (Stewart et al. *in preparation*).
450 Perhaps this process operates more effectively at warmer temperatures. The net outcome of the
451 tug of war is clear: infectivity depends more strongly on rearing temperature (Fig. 2C). Thus, in
452 warmer conditions parasites produce higher quality spores, and this process is the primary
453 determinant of spore infectivity.

454 Once we quantified the competing effects of temperature on infectivity, we could predict

the otherwise confusing response of transmission rate in our experiment. More specifically, transmission rate (β) responded in a complex way to the factorial combinations of parasite rearing temperature (T_R) and exposure/infection temperature (T_{EI}) due to tension between the three thermal effects (T_R on infectivity [u], T_{EI} on infectivity, and T_{EI} on foraging [f]; Fig. 2D, Table 2). Declines in rearing temperature dropped transmission overall because cold-reared spores were less infectious (producing contour means in Fig. 2D). However, hosts encounter spores while foraging (Hall et al. 2007), and foraging scales almost exponentially with temperature (within this thermal range). Thus, exposure pulls transmission up with temperature when spores are high quality (i.e., warm-reared). But, when spores are low quality (i.e., cold-reared), the rearing effect enhances the (linearly) declining component of exposure/infection temperature on infectivity, causing transmission rate to flatten (producing different contour slopes in Fig. 2D). Therefore, transmission rate depends on the net contributions of these three, competing thermal effects.

The thermal response of foraging rate (f) driving disease transmission via host-parasite contact is potentially a general mechanism. Metabolic rate increases with body temperature (Kooijman 2009). Therefore, foraging rate of poikilotherms must also increase with environmental temperature to accommodate the higher demand for energy (before dropping off at stressful, too-hot temperatures; Dell et al. 2014). However, empirical evidence for the thermal response of foraging rate scaling up to influence disease outcomes is mixed. Outbreak size increased with temperature for armyworms that consumed more baculovirus particles on leaves (Elderd and Reilly 2014), but transmission rate plateaued at high temperatures for a bacterial pathogen of *Daphnia* consumed during host foraging (Vale et al. 2008). For vector-borne diseases, the biting rate of arthropod vectors increases with temperature and contributes to the thermal response of disease; however, transmission is constrained by other traits at high temperatures, leading to intermediate peaks in transmission rate (Mordecai et al. 2013, 2017). Further investigation in more systems is needed to determine the generality of temperature-dependent exposure via foraging as a mechanism for the thermal response of disease.

Using a mathematical population model parameterized for the plankton system, we found that mean rearing temperature should closely track exposure/infection temperature during epidemics (Figs. 4A and Appendix S1: Fig. S2A). The lag between rearing and infection temperatures is small because lakes cool gradually due to the large volume of water and water's

high heat capacity. This finding simplifies the effect of temperature in the field for our system: warmer temperatures should increase transmission due to the net effect on infectivity (via the dominant parasite rearing effect) and exposure effects (via host foraging). Correspondingly, autumnal cooling should drop transmission rate and lead to the seasonal waning of epidemics (Fig. 4). However, the population model also shows that other outcomes are possible. For instance, substantial lags arise if temperature changes suddenly (see Appendix S1: Fig. S3), as can occur in terrestrial or smaller-volume aquatic habitats. Thus, the modeling approach used here could be applied to systems with thermal rearing effects but more abruptly-changing temperature though time.

The thermal response of transmission rate (*ß*) could have important implications for the seasonality of the fungal epidemics in *Daphnia*. We show some possibilities using simulations that illustrate how the thermal sensitivity of transmission rate can shape the size and timing of peak prevalence of epidemics. For instance, warmer starting conditions lead to larger epidemics which may or may not peak later in the season. These seasonal effects arise largely through an interplay between two temperature-dependent processes: the burn-through of susceptible hosts, *S*, and the change in the minimal host requirement for parasites, S^*. However, these simulations employ an all-else-equal approach: they assume that the initial starting conditions remain constant among scenarios (Figs. 4, 5, Appendix S1: Fig. S5). Epidemics vary substantially in their start date (and other characteristics) based on a variety of other ecological factors, such as dissolved organic carbon that blocks solar radiation (Overholt et al. 2012), zooplankton species that dilute disease (Penczykowski et al. 2014a, Strauss et al. 2015), and fish predation (Hall et al. 2006). These factors complicate mapping of predictions from our simple temperature-dependent model to field epidemics. (Hence, we have not yet attempted to do so here.)

These complicating ecological factors do interact with thermally-dependent transmission, however. When epidemics start later, they begin in cooler conditions. Thus, they are slowed by less infectious spores (rearing effect) and a lower exposure (foraging) rate. This idea is supported by evidence showing that epidemics that begin earlier (in warmer conditions) become much larger (Overholt et al. 2012, Penczykowski et al. 2014a, Shocket et al. 2018). Therefore, any factor inhibiting the start of epidemics, all else equal, should make them smaller via thermal effects describe here. Additionally, the simulations here demonstrate that temperature-dependent transmission and autumnal cooling can help explain why infection prevalence stereotypically

decreases during late fall: declining spore infectivity and host exposure in colder waters can terminate epidemics (Fig. 4, 5, Appendix S1: Fig. S5). This epidemic-ending mechanism may join others, including rapid evolution of host resistance (Duffy and Sivars-Becker 2007, Duffy et al. 2009), increases in density of diluters (Hall et al. 2009a), and declines in spore production at cold temperatures (Shocket et al. 2018). Future work will need to determine the relative contributions of temperature and other interacting drivers of epidemic start date, size, and seasonality.

The generality of rearing effects on parasites remains unclear. Only one other study has evaluated thermal rearing effects on parasite infectivity or virulence (Little et al. 2007). It did not detect a quality-mediated effect like the one shown here (i.e., warmer conditions yielding higher quality spores). That study (Little et al. 2007) also proposed (but did not find) an alternative mechanism for thermal rearing effects: acclimation. In an acclimation effect, performance should peak when past and current conditions match (Bennett and Lenski 1997, Little et al. 2007). A temperature matching pattern clearly did not emerge here either (i.e., there was no ridge of highest infectivity at matching T_R and T_{EI} in Fig. 2C). Instead, our findings echo another quality-type rearing effect in this plankton-fungus system. Certain host genotypes produce more infectious spores than others (i.e., a genotype rearing effect), and the parasite does not acclimate to host genotype (Searle et al. 2015). Thus, some environments simply provide higher quality conditions for rearing infectious parasites (e.g., warmer temperatures [here], specific host genotypes [Searle et al. 2015]). In other systems, better nutritional resources for previous hosts can render parasites more harmful (a protozoan parasite of mosquitoes: Tseng 2006; a bacterial parasite of *Daphnia*: Little et al. 2007) or less harmful (avian malaria: Cornet et al. 2014). Rearing effects of algal resources—if found in this system—could also drive seasonality or heterogeneity of disease since resources often vary seasonally (Hall et al. 2009b) or between lakes (Civitello et al. 2015). Furthermore, co-varying seasonal changes in algal resources and temperature could jointly influence transmission via rearing effects. Therefore, rearing effects on parasite infectivity could influence epidemics in this plankton system, and potentially others, in under-evaluated ways.

Thus, we hope that this planktonic example can inspire more work on rearing effects. Rearing effects provide a mechanistically distinct influence on parasites, and hence epidemics. Further, rearing effects of all types—thermal, nutritional, and host genotype—remain

understudied. Thus, they could drive parasite performance and disease seasonality to an underappreciated extent. Rearing effects are most likely to emerge for parasites with short infection cycles that multiply repeatedly during epidemics. They also likely require that environmental conditions change at longer temporal scales relative to parasite reproduction and spread. Additionally, three of four disease systems with documented rearing effects involve eukaryotic parasites (the other is bacterial). We need more factorial experiments that dissect parasite plasticity, i.e., those which can distinguish between the effects of rearing versus current environments on parasite traits (see Appendix for a note on experimental designs). However, an experimental search for rearing effects must also separate plasticity from evolutionary effects. The focal fungus here shows no observed genetic variation for infectivity in experiments (Duffy and Sivars-Becker 2007, Auld et al. 2014, Searle et al. 2015). Hence, we illustrate a solely plastic effect. Other parasites can evolve very rapidly (Ebert 1998, Altizer et al. 2003). In those systems, genotypic changes must be separated from plastic rearing effects. With that caveat in mind, we hope that careful evaluation across more host-parasite systems will determine the generality of these plastic rearing effects and their potential contribution to seasonal epidemics.

ACKNOWLEGMENTS

K. Boatman assisted with 2010 field sampling. ATS, JMW, and MSS were supported by the NSF GRFP. JLH was supported by an EPA STAR fellowship. This work was supported in part by NSF DEB 0841679, 0841817, 1120316, 1120804, 1353749, 1354407, and 1353806. Competing interest: DV is the founder and president of the non-profit Agricultural Genomics Foundation.

LITERATURE CITED

Adamo, S. A., and M. M. E. Lovett. 2011. Some like it hot: the effects of climate change on reproduction, immune function and disease resistance in the cricket *Gryllus texensis*. Journal of Experimental Biology 214:1997–2004.

Altizer, S., A. Dobson, P. Hosseini, P. Hudson, M. Pascual, and P. Rohani. 2006. Seasonality and the dynamics of infectious diseases. Ecology Letters 9:467–84.

Altizer, S., D. Harvell, and E. Friedle. 2003. Rapid evolutionary dynamics and disease threats to biodiversity. Trends in Ecology and Evolution 18:589–596.

579 Auld, S. K., S. R. Hall, J. Housley Ochs, M. Sebastian, and M. A. Duffy. 2014. Predators and
580 patterns of within-host growth can mediate both among-host competition and evolution of
581 transmission potential of parasites. American Naturalist 184:S77-90.
582 Ben-Ami, F., D. Ebert, and R. R. Regoes. 2010. Pathogen dose infectivity curves as a method to
583 analyze the distribution of host susceptibility: a quantitative assessment of maternal effects
584 after food stress and pathogen exposure. The American Naturalist 175:106–115.
585 Bennett, A. F., and R. E. Lenski. 1997. Evolutionary Adaptation to Temperature . VI .
586 Phenotypic Acclimation and Its Evolution in Escherichia coli. Evolution 51:36–44.
587 Bolker, B. M., and R Development Core Team. 2017. bbmle: Tools for General Maximum
588 Likelihood Estimation.
589 Boots, M., and K. E. Roberts. 2012. Maternal effects in disease resistance: poor maternal
590 environment increases offspring resistance to an insect virus. Proceedings of the Royal
591 Society B: Biological Sciences 279:4009–4014.
592 Civitello, D. J., R. M. Penczykowski, A. N. Smith, M. S. Shocket, M. A. Duffy, and S. R. Hall.
593 2015. Resources, key traits and the size of fungal epidemics in Daphnia populations. Journal
594 of Animal Ecology 84:1010–1017.
595 Cornet, S., C. Bichet, S. Larcombe, B. Faivre, and G. Sorci. 2014. Impact of host nutritional
596 status on infection dynamics and parasite virulence in a bird-malaria system. Journal of
597 Animal Ecology 83:256–265.
598 Dell, A. I., S. Pawar, and V. M. Savage. 2014. Temperature dependence of trophic interactions
599 are driven by asymmetry of species responses and foraging strategy. Journal of Animal
600 Ecology 83:70–84.
601 Duffy, M. A., S. R. Hall, A. J. Tessier, and M. Huebner. 2005. Selective predators and their
602 parasitized prey: Are epidemics in zooplankton under top-down control? Limnology and
603 Oceanography 50:412–420.
604 Duffy, M. A., and L. Sivars-Becker. 2007. Rapid evolution and ecological host-parasite
605 dynamics. Ecology Letters 10:44–53.
606 Duffy, M., S. Hall, C. Cáceres, and A. Ives. 2009. Rapid evolution, seasonality, and the
607 termination of parasite epidemics. Ecology 90:1441–1448.
608 Ebert, D. 1998. Experimental Evolution of Parasites. Science 282:1432–1436.
609 Ebert, D. 2005. Ecology, epidemiology, and evolution of parasitism in *Daphnia*. National

Library of Medicine (USA), Center for Biotechnology Information, Bethesda.
Elderd, B. D., and J. R. Reilly. 2014. Warmer temperatures increase disease transmission and outbreak intensity in a host-pathogen system. Journal of Animal Ecology 83:838–849.
Fuller, C. A., M. A. Postava-Davignon, A. West, and R. B. Rosengaus. 2011. Environmental conditions and their impact on immunocompetence and pathogen susceptibility of the Caribbean termite Nasutitermes acajutlae. Ecological Entomology 36:459–470.
Garbutt, J. S., J. A. Scholefield, P. F. Vale, and T. J. Little. 2014. Elevated maternal temperature enhances offspring disease resistance in *Daphnia magna*. Functional Ecology 28:424–431.
Grassly, N. C., and C. Fraser. 2006. Seasonal infectious disease epidemiology. Proceedings of the Royal Society B: Biological Sciences 273:2541–50.
Green, J. 1974. Parasites and epibionts of Cladocera. The Transactions of the Zoological Society of London 32:417–515.
Hall, S. R., C. R. Becker, M. A. Duffy, and C. E. Cáceres. 2011. Epidemic size determines population-level effects of fungal parasites on Daphnia hosts. Oecologia 166:833–842.
Hall, S. R., C. R. Becker, J. L. Simonis, M. A. Duffy, A. J. Tessier, and C. E. Cáceres. 2009a. Friendly competition: Evidence for a dilution effect among competitors in a planktonic host-parasite system. Ecology 90:791–801.
Hall, S. R., C. J. Knight, C. R. Becker, M. A. Duffy, A. J. Tessier, and C. E. Cáceres. 2009b. Quality matters: resource quality for hosts and the timing of epidemics. Ecology Letters 12:118–128.
Hall, S. R., L. Sivars-Becker, C. Becker, M. A. Duffy, A. J. Tessier, and C. E. Cáceres. 2007. Eating yourself sick : transmission of disease as a function of foraging ecology. Ecology Letters 10:207–218.
Hall, S. R., R. Smyth, C. R. Becker, M. A. Duffy, C. J. Knight, S. MacIntyre, A. J. Tessier, and C. E. Cáceres. 2010. Why Are Daphnia in Some Lakes Sicker? Disease Ecology, Habitat Structure, and the Plankton. BioScience 60:363–375.
Hall, S. R., A. J. Tessier, M. A. Duffy, M. Huebner, and C. E. Cáceres. 2006. Warmer does not have to mean sicker: temperature and predators can jointly drive timing of epidemics. Ecology 87:1684–95.
Holeski, L. M., G. Jander, and A. A. Agrawal. 2012. Transgenerational defense induction and epigenetic inheritance in plants. Trends in Ecology and Evolution 27:618–626.

641 Kooijman, S. A. L. M. 2009. Dynamic Energy Budget Theory for Metabolic Organisation. Third
642 edition. Cambridge University Press, New York, New York.
643 Lazzaro, B. P., and T. J. Little. 2009. Immunity in a variable world. Philosophical transactions of
644 the Royal Society of London. Series B, Biological sciences 364:15–26.
645 Linder, J. E., K. A. Owers, and D. E. L. Promislow. 2008. The effects of temperature on host-
646 pathogen interactions in *D. melanogaster*: Who benefits? Journal of Insect Physiology
647 54:297–308.
648 Little, T., J. Birch, P. Vale, and M. Tseng. 2007. Parasite transgenerational effects on infection.
649 Evolutionary Ecology Research 9:459–469.
650 McCallum, H., A. Fenton, P. J. Hudson, B. Lee, B. Levick, R. Norman, S. E. Perkins, M. Viney,
651 A. J. Wilson, and J. Lello. 2017. Breaking beta: deconstructing the parasite transmission
652 function. Philosophical Transactions of the Royal Society B: Biological Sciences
653 372:20160084.
654 Metschnikoff, E. 1884. A disease of *Daphnia* caused by a yeast. A contribution to the theory of
655 phagocytes as agents for attack on disease-causing organisms. Archiv. Path. Anat. Phys.
656 Klin. Med. 96:177–195.
657 Mideo, N., and S. E. Reece. 2012. Plasticity in parasite phenotypes: evolutionary and ecological
658 implications for disease. Future Microbiology 7:17–24.
659 Mitchell, S. E., and A. F. Read. 2005. Poor maternal environment enhances offspring disease
660 resistance in an invertebrate. Proceedings of the Royal Society B: Biological Sciences
661 272:2601–2607.
662 Mordecai, E. A., J. M. Cohen, M. V. Evans, P. Gudapati, L. R. Johnson, C. A. Lippi, K.
663 Miazgowicz, C. C. Murdock, J. R. Rohr, S. J. Ryan, V. Savage, M. S. Shocket, A. Stewart
664 Ibarra, M. B. Thomas, and D. P. Weikel. 2017. Detecting the impact of temperature on
665 transmission of Zika, dengue, and chikungunya using mechanistic models. PLOS Neglected
666 Tropical Diseases 11:e0005568.
667 Mordecai, E. A., K. P. Paaijmans, L. R. Johnson, C. Balzer, T. Ben-Horin, E. de Moor, A.
668 McNally, S. Pawar, S. J. Ryan, T. C. Smith, and K. D. Lafferty. 2013. Optimal temperature
669 for malaria transmission is dramatically lower than previously predicted. Ecology letters
670 16:22–30.
671 Moret, Y. 2006. “Trans-generational immune priming”: specific enhancement of the

antimicrobial immune response in the mealworm beetle, Tenebrio molitor. Proceedings of the Royal Society B: Biological Sciences 273:1399–405.

Murdock, C. C., K. P. Paaijmans, A. S. Bell, J. G. King, J. F. Hillyer, A. F. Read, and M. B. Thomas. 2012. Complex effects of temperature on mosquito immune function. Proceedings. Biological sciences / The Royal Society 279:3357–3366.

Ouedraogo, R. M., M. Cusson, M. S. Goettel, and J. Brodeur. 2003. Inhibition of fungal growth in thermoregulating locusts, *Locusta migratoria*, infected by the fungus <i>Metarhizium anisopliae var acridum<i/>. Journal of Invertebrate Pathology 82:103–109.

Overholt, E. P., S. R. Hall, C. E. Williamson, C. K. Meikle, M. A. Duffy, and C. E. Cáceres. 2012. Solar radiation decreases parasitism in Daphnia. Ecology Letters 15:47–54.

Pascual, M., and A. Dobson. 2005. Seasonal patterns of infectious diseases. PLoS Medicine 2:0018–0020.

Penczykowski, R. M., S. R. Hall, D. J. Civitello, and M. A. Duffy. 2014a. Habitat structure and ecological drivers of disease. Limnology and Oceanography 59:340–348.

Penczykowski, R. M., B. C. P. Lemanski, R. D. Sieg, S. R. Hall, J. Housley Ochs, J. Kubanek, and M. A. Duffy. 2014b. Poor resource quality lowers transmission potential by changing foraging behaviour. Functional Ecology 28:1245–1255.

R Core Team. 2017. R: A language and for statistical computing. R Foundation for Statistical Computing, Vienna, Austria.

Sadd, B. M., Y. Kleinlogel, R. Schmid-Hempel, and P. Schmid-Hempel. 2005. Trans-generational immune priming in a social insect. Biology Letters 1:386–388.

Sarnelle, O., and A. E. Wilson. 2008. Type III functional response in *Daphnia*. Ecology 89:1723–1732.

Searle, C. L., J. H. Ochs, C. E. Cáceres, S. L. Chiang, N. M. Gerardo, S. R. Hall, and M. A. Duffy. 2015. Plasticity, not genetic variation, drives infection success of a fungal parasite. Parasitology 142:839–848.

Shocket, M. S., A. T. Strauss, J. L. Hite, M. Šljivar, D. J. Civitello, M. A. Duffy, C. E. Cáceres, and S. R. Hall. 2018. Temperature Drives Epidemics in a Zooplankton-Fungus Disease System: A Trait-Driven Approach Points to Transmission via Host Foraging. The American Naturalist 191:435–451.

Strauss, A. T., D. J. Civitello, C. E. Cáceres, and S. R. Hall. 2015. Success, failure and ambiguity

of the dilution effect among competitors. Ecology Letters 18:916–926.
Tessier, A. J., and P. Woodruff. 2002. Cryptic trophic cascade along a gradient of lake size. Ecology 83:1263–1270.
Triggs, A., and R. J. Knell. 2012. Interactions between environmental variables determine immunity in the Indian meal moth Plodia interpunctella. Journal of Animal Ecology 81:386–394.
Tseng, M. 2006. Interactions between the parasite's previous and current environment mediate the outcome of parasite infection. The American Naturalist 168:565–571.
Vale, P. F., M. Stjernman, and T. J. Little. 2008. Temperature-dependent costs of parasitism and maintenance of polymorphism under genotype-by-environment interactions. Journal of Evolutionary Biology 21:1418–1427.
Wolinska, J., S. Giessler, and H. Koerner. 2009. Molecular identification and hidden diversity of novel Daphnia parasites from European lakes. Applied and Environmental Microbiology 75:7051–7059.
Wolinska, J., and K. C. King. 2009. Environment can alter selection in host-parasite interactions. Trends in Parasitology 25:236–244.

DATA AVAILABILITY

Data associated with this study are available from the Dryad Digital Repository: https://doi.org/10.5061/dryad.g22t8m0

Table 1: Traits for the temperature-dependent model of transmission rate (Fig 1B). Coefficients (with 95% confidence intervals from bootstrapping) are given for traits fit as functions of temperature. All functions were fit with temperature in Kelvin.

Function	Meaning (units)	Function Type	Function Coefficients (95% CIs)[a]

f (eq. 1)	host foraging rate (L / day)	Arrhenius function of T_{EI} with power function of body length (L): $f(T_{EI}, L) = L^{\gamma} \cdot \hat{f} \cdot e^{T_A\left(\frac{1}{T_{Ref}} - \frac{1}{T_R}\right)}$	γ = **2.18** (1.60 – 2.98) $\hat{f}$ = **5.36 · 10^{-3}** (3.70 – 6.75 · 10^{-3}) T_A = **8,720** (4,800 – 12,600)
u (eq. 2)	Per spore infectivity ($spore^{-1}$)	Linear function of T_{EI} and T_R: $u(T_{EI}, T_R) = \alpha_{EI} T_{EI} + \alpha_R T_R + \alpha_I$	α_{EI} = **-4.93 · 10^{-5}** (-10.3 – -1.08 · 10^{-5}) α_R = **8.99 · 10^{-5}** (6.89 – 12.1 · 10^{-5}) α_I = **-0.0111** (-0.0245 – 0.00188)

[a] Coefficients (units): γ: exponent (unitless); f_R: foraging at reference temperature (L mm$^{-\gamma}$ day^{-1}); T_{Ref}: reference temperature (20°C = 293.15 K); T_A: Arrhenius temperature (K); α_{EI} and α_R: slope coefficients (spore^{-1} K^{-1}); α_I: intercept (spore^{-1})

Table 2: A qualitative summary of the results for the temperature-dependent model of transmission rate (Fig. 2). The effect of rearing temperature (T_R) on spore infectivity (u) alters the net balance between the two opposing influences of exposure/infection temperature (T_{EI}): the increasing component due to foraging (f) and the declining component on infectivity. Collectively, these three mechanisms determine the transmission rate (ß).

T_R / T_{EI} temperatures	**Sign of thermal effect on transmission rate for each mechanism:**			**Net transmission rate (ß)**
	T_R on spore infectivity (u)	*T_{EI} on spore infectivity (u)*	*T_{EI} on foraging (f)*	
Warm / Warm	+	-	+	High
Warm / Cool	+	+	-	Medium
Cool / Warm	-	-	+	Low
Cool / Cool	-	+	-	Low

FIGURE LEGENDS

Figure 1: A transmission model that depends on rearing (T_R) and exposure/infection (T_{EI}) temperatures. (A) Example of a typical epidemic (Downing Lake in 2010; infection prevalence in black). Weighted temperature (in aqua; the effective temperature that hosts experience based on daily migration patterns) decreases over the epidemic season (late summer to early winter).

Thus, hosts encounter parasites in a seasonally cooling thermal environment. (B) Transmission rate (β) is the product of host foraging (exposure) rate, $f(T_{EI})$ (eq. 1), and spore infectivity, $u(T_{EI},T_R)$ (eq. 2). Host foraging rate only depends on exposure/infection temperature and host physiology. Spore infectivity depends on both temperatures. T_{EI} influences spore infectivity via host and parasite physiology, while T_R only determines the baseline infectivity of spores.

Figure 2: Parameterization of the transmission model (A, B) Host foraging rate, $f(T_{EI}, L)$: (A) Points from foraging assay, across body length (L) and temperature (T_{EI}) gradients. Lines show the parameterized model (eq. 1). (B) Foraging rate model parameterized for large adults in infection assay (length [L] = 1.5 mm; thick solid line) and for population average in simulations (L= 0.85 mm; thick dashed line; thin lines are 95% confidence intervals). (C) Spore infectivity, $u(T_{EI},T_R)$, fit as a plane dependent on rearing temperature (T_R, light gray arrows) and exposure/infection temperatures (T_{EI}, dark gray arrows, eq. 2). The dashed line approximates the trajectory of lake temperature during the epidemic season. Colors indicate rearing temperatures: dark red = 22°C, light red = 20°C, light blue = 18°C, dark blue = 15°C. (D) Transmission rate, $\beta(T_{EI},T_R)$: Empirical estimates from the infection assay (dashed lines connecting points) and model-predicted transmission (solid lines). Error bars omitted for visual clarity (included in Appendix S1: Fig. S1). Circles around points denote treatments where $T_{EI} \approx T_R$ (i.e., no lag between T_{EI} and T_R). Colors are same rearing temperatures as in panel C.

Figure 3: The infectivity of spores collected from natural epidemics (indexed by transmission rate: see text) decreased with rearing temperature in two of three lakes (Gambill $p < 0.0001$, Clear $p = 0.0024$), with a non-significant trend in Scott ($p = 0.16$). '*' and 'NS' denote significant and non-significant P-values, respectively. Error bars are 95% CIs based on 10,000 bootstraps.

Figure 4: Simulated epidemics (eq. 3) with a single scenario of seasonal cooling and factorial combinations of temperature-dependent components of transmission rate. (A) Exposure/infection temperature (T_{EI}) changes sigmoidally (eq. 3e; T_{max} = maximum temperature, T_{min} = minimum temperature, R = cooling rate, and D = day when temperature reaches midpoint; T_{max} = 25°C, R = 1.06, D = 70, and T_{min} = 15°C). The difference between spore rearing temperature (T_R; aqua, solid line) and T_{EI} (black, dashed lines) was negligible, peaking at ~0.17°C in all simulations.

(B) Transmission rate and (C) infection prevalence during epidemics. Host foraging rate (f) and per spore infectivity (u) are held constant at the hottest value (at 25°C) or varied as functions of T_{EI} and T_R: both traits constant (solid black line), thermally-dependent u only (solid purple line), thermally-dependent f only (dashed black line), and both traits thermally-dependent (dashed purple line). Foraging rate has a larger effect, but both traits contribute to waning epidemics as temperatures cool.

Figure 5: Simulated epidemics with multiple scenarios of seasonal cooling and all traits as temperature-dependent functions. Top row varies starting temperature (T_{max}), middle row varies start date of cooling (D), and bottom row varies cooling rate (R). Left column shows five cooling scenarios, middle column shows corresponding epidemic dynamics, and right column shows how two epidemic properties (size and date of peak prevalence) vary with each parameter. Points in the right column correspond to the five examples in the first two columns. Parameters values decrease as lines become less solid and colors become more cool (i.e., red >orange > green > blue > purple). (A,B,C) Starting temperature, T_{max}: epidemics are larger with hotter starting temperatures. Epidemics reach peak prevalence later at intermediate starting temperatures. (D,E,F) Start date of cooling: epidemics are larger and peak later as start date of cooling moves later in the season. (G,H,I) Cooling rate, R: epidemic properties are relatively stable with varying cooling rates. Base cooling parameters: T_{max} = 25°C, D = 70, R = 1.06, and T_{min} = 15°C.

A

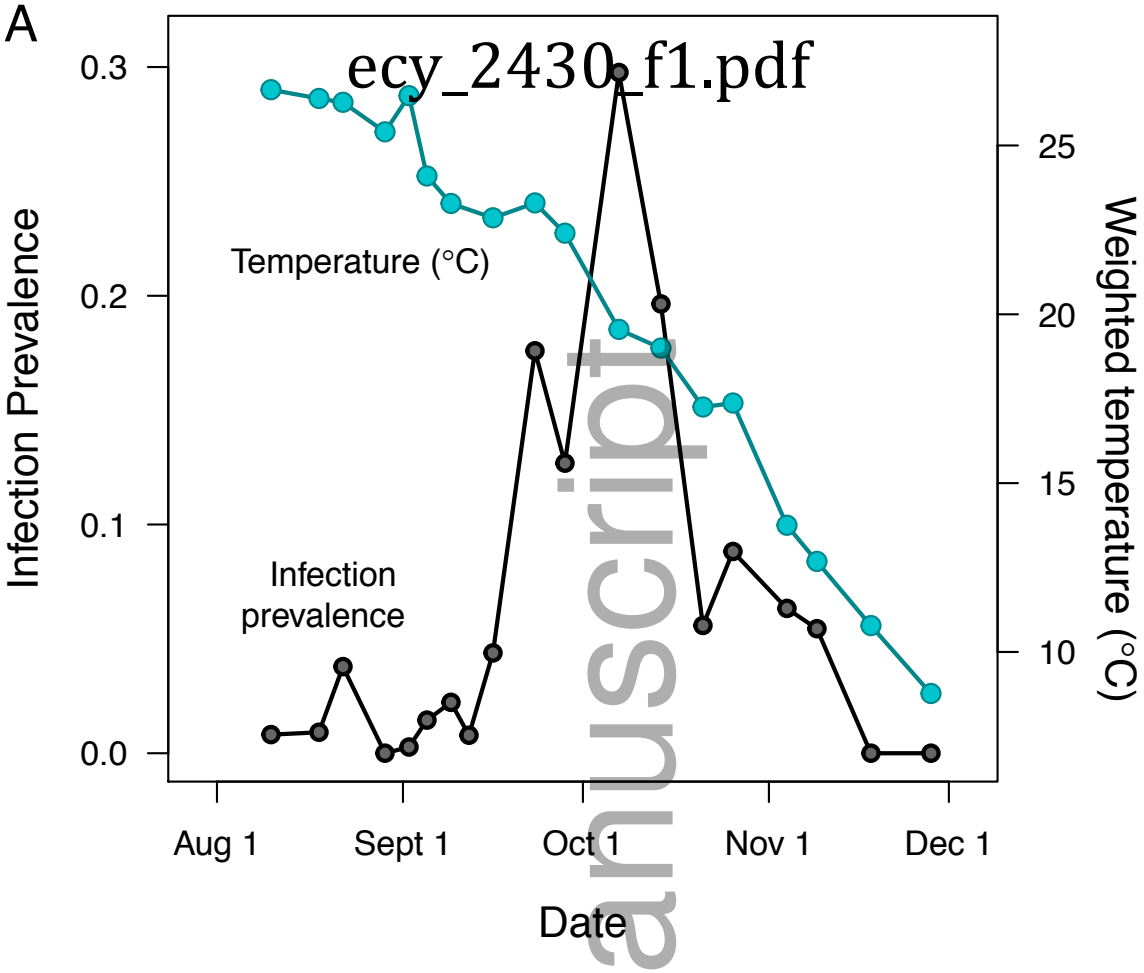

B

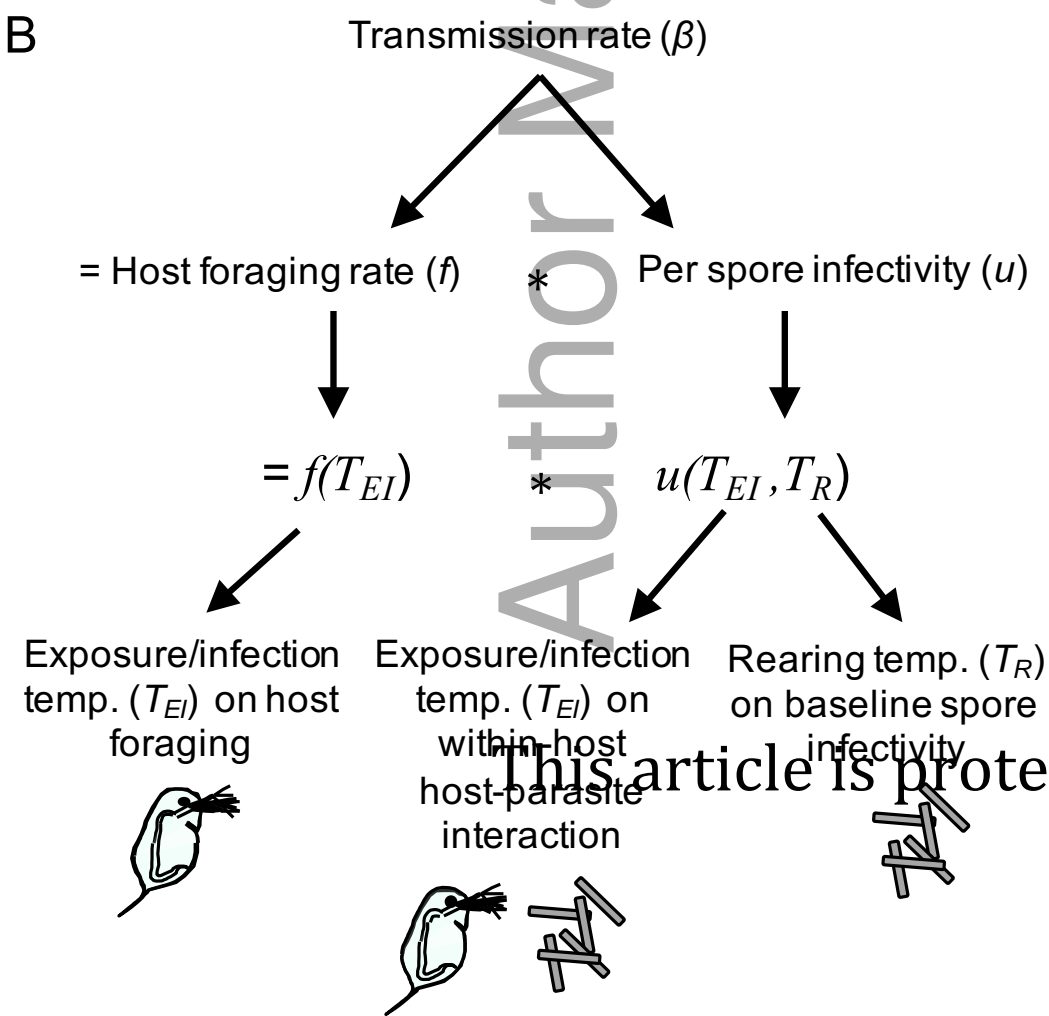

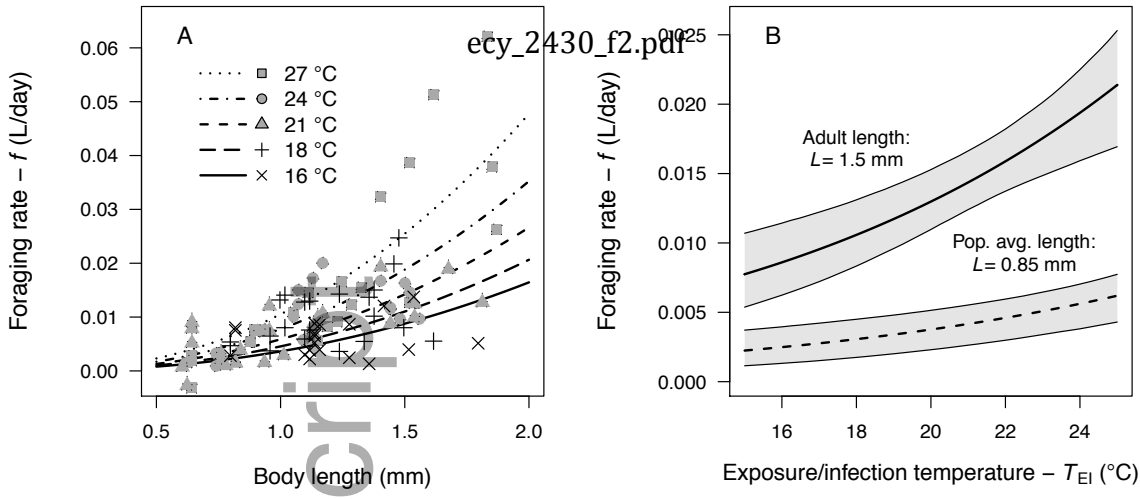

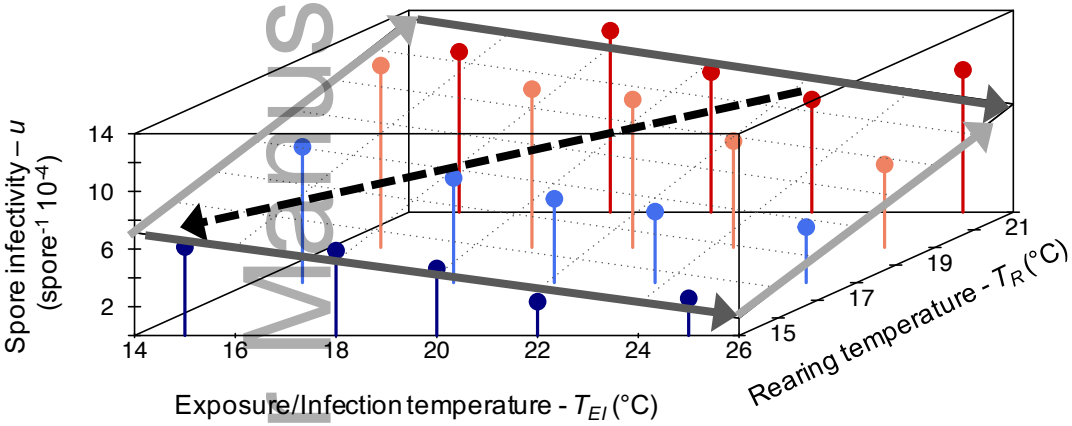

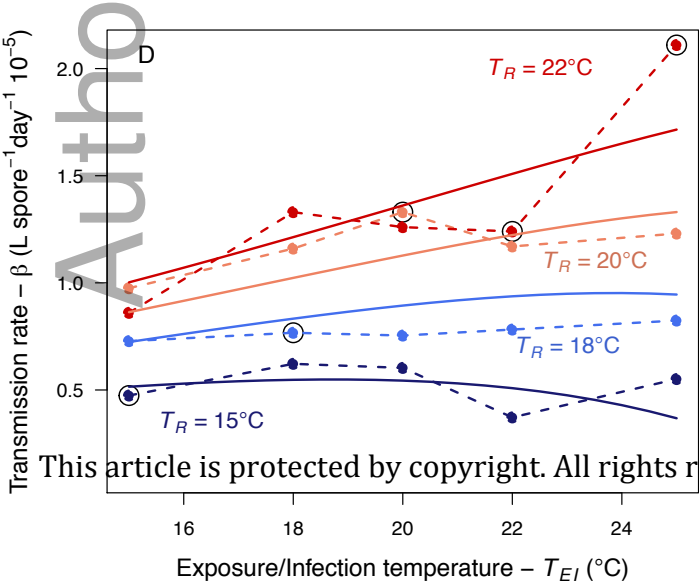

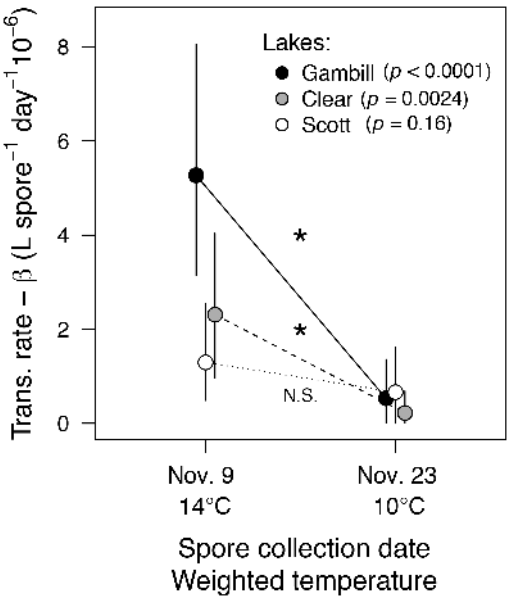

ecy_2430_f3.tif